Heliyon 6 (2020) e03320

Contents lists available at ScienceDirect

Heliyon

journal homepage: www.cell.com/heliyon

Research article

Interpretation of high resolution aeromagnetic data of Kaoje and its environ, western part of the Zuru Schist belt, Nigeria: implication for Fe–Mn occurrence

Nurudeen Olasunkanmi [a,*], Olufemi Bamigboye [b], Olatunji Saminu [c], Naheem Salawu [d], Toba Bamidele [b]

[a] Physics and Materials Science Department, Kwara State University, Malete, Nigeria
[b] Department of Geology and Mineral Science, Kwara State University, Malete, Nigeria
[c] Department of Geophysics, University of Ilorin, Ilorin, Nigeria
[d] BS Geophysical and Consultancy Ltd, Nigeria

ARTICLE INFO

Keywords:
Physics
Geophysics
Environmental science
Earth sciences
Geochemistry
Manganite
Goethite
Fault
Mineralization potential
Magnetic anomalies
Schist belt

ABSTRACT

This study presents an appraisal of mineralization potential and the geologic record of Kaoje and environs using high-resolution aeromagnetic data. The data were analyzed using the fast Fourier transform technique for reduction-to-equator (RTE), analytic signal (AS), total horizontal derivative (THDR), tilt derivative (TDR), spectral analysis and Euler deconvolution at varying spectral indices. The reduced to equator residual magnetic intensity range from -73.4 to 205.6 nT and are associated with contrasting lithology of the Sedimentary and Basement Complex rocks. The anomalies and analytic signal amplitude unfold and update the extension of Zuru Schist to the southern region of Kaoje, elongated banded gneiss within the schist body, pegmatite intrusion through the migmatite and NNW-SSE trending schist hosted manganite and sandstone-hosted goethite. Estimated depth to shallow and deeper magnetic sources ranged from 0 to 59 m and 225–415 m respectively, and the corresponding Euler solutions revealed perfect clustering along notable geologic features and minerals. The iron mineralization are revealed as sourced from the magmatic bodies that lie beneath the sedimentary rocks and a corresponding sphere geologic model within northwest and southwest of Kaoje at a depth range of 0–225 m. The structural trends suggested the tectonic events in the area and indicate an imprint of Zungeru-Anka transcurrent fault that serves as a conduit for iron mineralizing fluid to Kaoje.

1. Introduction

Solid mineral exploration using the traditional geological methods of field mapping, direct visual observation, sampling, and geochemical analysis have yielded a very good results in the last century. Some of the results include but not limited to working exploration models, understanding of the geology and mechanism of ore deposit formations, reserve estimation among others. However, the constraint in the discovery of new ore deposits have necessitated a shift in exploratory activities from the conventional geological methods to integrated exploration wherein remote sensing techniques and geochemical methods are incorporated with geological methods (Ibrahim et al., 2016).

Magnetic data are frequently used in direct detection of mineralization (such as iron-ore deposits and heavy mineral sands), for locating favorable host rocks such as carbonites, kimberlite, porphyritic intrusion, faulting and hydrothermal alteration, and for mapping geologic features of prospective areas (Roux, 1970; Macnae, 1979; Keating, 1995; Chapin *et al.*, 1998; Power et al., 2004; Amigun et al., 2012). Faults are recognized by magnetic minerals that are oxidized to non-magnetic minerals along a fault plane or a linear narrow magnetic low caused by weathering along the fault plane. These can have similar magnetic expression as joints that can serve as conduits for mineralizing fluid. Application of integrated analytical tools to magnetic data residualization within frequency domain using fast Fourier transform enhances the resolution of anomalies associated with geologic features that can be interpreted for desired purposes (Nureddin et al., 2008; Paananen, 2013; Olasunkanmi et al., 2017). Minerals occur in three main metallogenic provinces viz: the Precambrian Basement Complex, the Jurassic Younger Granites and

* Corresponding author.
E-mail address: nurudeen.olasunkanmi@kwasu.edu.ng (N. Olasunkanmi).

https://doi.org/10.1016/j.heliyon.2020.e03320
Received 25 February 2019; Received in revised form 25 June 2019; Accepted 24 January 2020
2405-8440/© 2020 Published by Elsevier Ltd. This is an open access article under the CC BY-NC-ND license (http://creativecommons.org/licenses/by-nc-nd/4.0/).

Cretaceous-Tertiary sedimentary basins (Akande and Kinnaird, 1992). These provinces are characterized by mineralizing fluids that vary between metamorphic origin, magmatic origin and connate water for the Precambrian, Jurassic and Cretaceous-Tertiary province respectively (Barton and Johnson, 2000).

Kaoje lies within the contact zone between the Cretaceous Sokoto sedimentary basin and the Basement Complex of Northwestern Nigeria (Obaje, 2009). It falls within the western region of Zuru schist belt, which is believed to be the largest and the least understood schist belt in northwestern Nigeria (Danbatta and Garba, 2007). The geothermal parameters of the area indicate low depth of magnetic sources and relatively low geothermal gradients (Nwankwo and Shehu, 2015). Kaoje has been identified to have goethite and manganite mineralizations (Akinlolu, 2007; Bamigboye et al., 2015, 2018). The goethites are hosted by sedimentary rocks while the manganites are schist hosted. In addition, the goethites are said to be of hydrothermal origin in contrast to the manganites that are of supergenetic origin. Bamigboye et al. (2018) added that the goethites were remobilized and now hosted by the sedimentary rocks as a result of changing environmental conditions. However, the mineralization are said to be structurally controlled. The mode of occurrence, depth to magnetic sources and the thickness of the sedimentary rocks that host the iron, and possible geologic records of what underlies the sedimentary rocks were not reported. Therefore, this work is conceptualized at appraising the mineralization potential of Kaoje using high resolution aeromagnetic and geologic data.

1.1. Geologic setting

The study area covers an approximate area of 851 square km between longitude 3° 54′ E to 4° 10′ E and latitude 11° 00′ N and11° 15′ N. It is at approximately 7 km west of Maje, a boundary community between the Republic of Benin and Nigeria. The geology of the area can be grossly

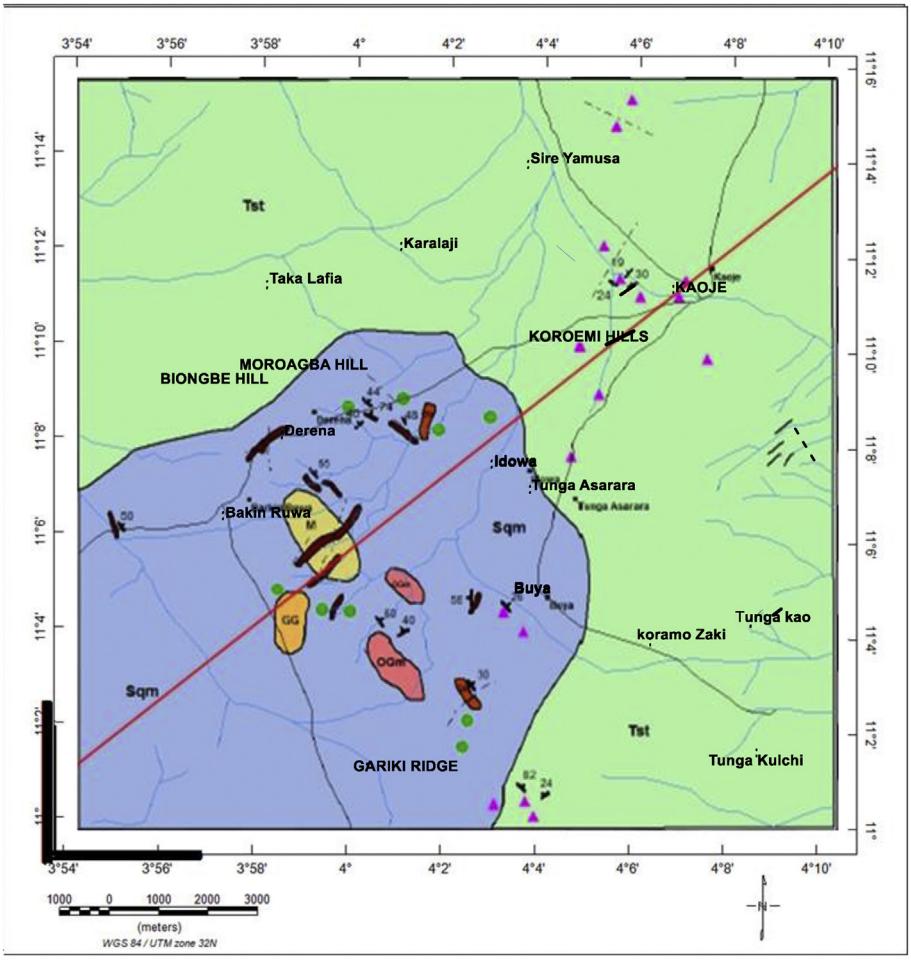


Figure 1. Geological Map of Kaoje and its environs (part of Kaoje sheet 94SE and Bani sheet 95SW) showing the mapped geological components (after: Bamigboye et al., 2018).

divided into the Basement Complex and the sedimentary rocks (Figure 1). The Basement Complex rocks are of the Precambrian age (Obaje, 2009) and comprise of Migmatite–Gneiss Complex, Older Granite and the schist. The Zuru Schist Belt is believed to be the largest and the least understood schist belt in Northwestern Nigeria (Danbatta and Garba, 2007; Fillie, 2014). The sedimentary rocks belong to the Sokoto/Lullemenden Basin and of the Taloka Formation, comprising of sandstone, siltstone, and claystone. This Basin is believed to have been formed by tectonic epirogenic movement or stretching and rifting of the tectonically stable crust during the Paleozoic (Ajibade et al., 1987). The age of the sediments in this basin reduces toward the SW from the north (Bassey and Eminue, 2014). These sedimentary rocks form most of the elevated features which include the Biongbe, Morongba and Koremi hills in the study area.

2. Data source and methodology

This study establishes the geometry, mode, and depth of occurrence of Fe–Mn mineralization in the western part of Zuru Schist Belt by integrating the dataset acquired from an airborne magnetic survey with geologic field observations. High-resolution aeromagnetic data (covering Kaoje and Bani; sheets 94 and 95 of magnetic index map of Nigeria) were obtained from Nigeria Geological Survey Agency (NGSA, 2006). The data were acquired between 2004 and 2009 by Fugro Airborne Survey Limited. It presented a magnetic total field at a data recording interval of 0.1 s using 3x-Scintrex CS3 Cesium Vapour magnetometer and at a flight height of 200 m. The geologic fieldwork carried out on a scale of 1:50, 000 involved lithologic mapping, in-situ rock sampling and petrographic analysis.

The magnetic data were: gridded at a mesh size of 50 m to reduce noise and enhance the resolution of anomalies (Patterson and Reeves, 1985), de-cultured, leveled and corrected for International Geomagnetic Reference Field. The filtered anomalies were reduced to magnetic equator in order to produce anomalies which depend on the inclination and declination of the body's magnetization, the local earth's field and orientation of the body with respect to the magnetic north. The study area lies within magnetic equatorial regions of low inclination (I = -8.59) where reduction to pole is not a valid technique; since N–S bodies have no detectable induced magnetic anomaly at zero geomagnetic inclination. Baranov (1957) defined a magnetic transformation that can convert complex asymmetric anomalies of intermediate latitude to a simple symmetric anomaly, characteristics of Polar Regions with a zero horizontal offset. Once the field has been reduced to the equator, the regional magnetic field align horizontally and most of the source magnetizations are horizontal (Foss, 2011; Ayodeji and Dare, 2015).

The resultant composite color depicting reduced-to-equator residual magnetic anomalies (Figure 2) are attributable to varying magnetic units in the area. The physical characteristics of some rock units within the area were sampled, prepared and examined under a petrographic microscope to analysis various optical properties such as relief, shape, and twinning. The magnetic anomalies were further enhanced using the fast Fourier transform an approach which involved Analytic Signal (AS), Tilt derivatives (TDR) and Total Horizontal (THDR), Source parameters and Euler deconvolution at varying spectral indices (Table 1) on Oasis Montaj geosoftware. These were carried out to examine the mode of occurrence and geologic structures associated with the modal composition of the rock units.

Analytic Signal (AS) approach used the total magnetic gradient to approximately estimate positions of magnetic contacts by mapping the source distribution at shallow levels (Nabighian, 1972; Roest et al., 1992). It is a vector sum of the three orthogonal derivatives (horizontal gradient (HDR) in the x-direction and in y-direction, and vertical gradient (VDR) as stated in Eq. (1) (where M is the total magnetic field) and as its amplitude (ASA) peaks over magnetic boundaries. Various attributes of

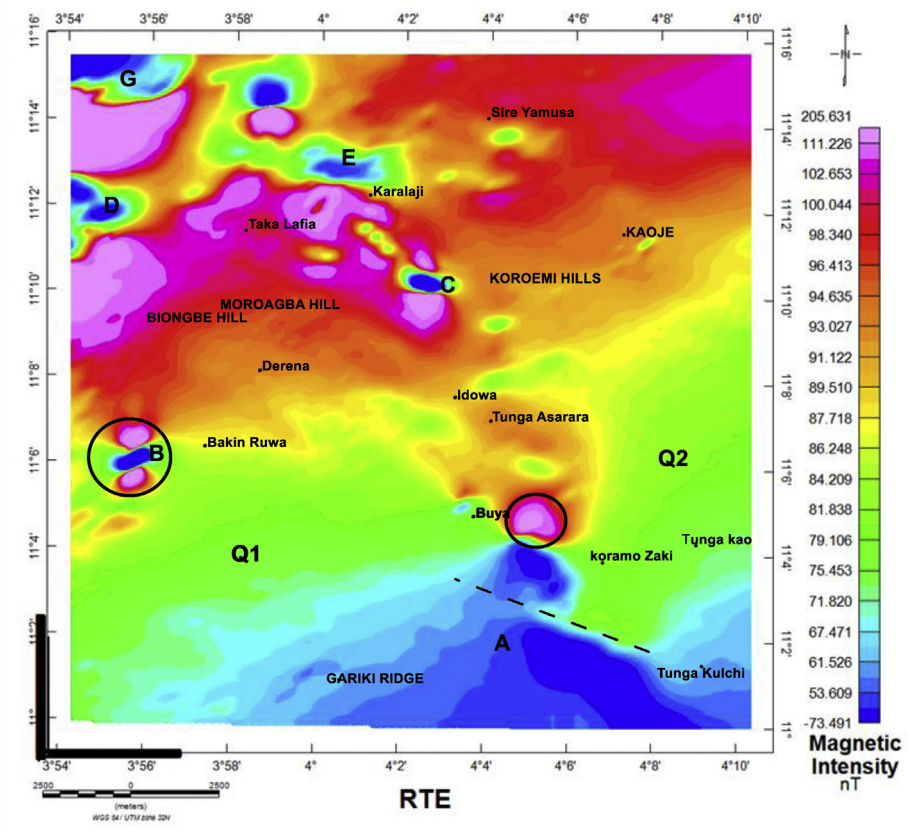


Figure 2. Color shaded reduced to equator (RTE) residual magnetic intensity map of the study area.

Table 1. Structural indices (SI) for various geological models and corresponding infinite dimensions (Thompson, 1982; Geosoft Incorporation, 2005).

Structural Index	Geological Model	Number of Infinite dimensions
0	Contact	3 (X, Y and Z)
1	Sill	2 (X and Y)
1	Dyke	2 (Z and X or Y)
2	Horizontal cylinder	1 (X or Y)
2	Pipe	1 (Z)
3	Sphere	0

the anomalies are revealed with distinct tone at the magnetic boundaries which corresponds to geologic units (such as lithological assemblage) in Figure 3. The source parameters were used to obtain some depth estimates using horizontal and vertical gradient components (Thurston et al., 1999), by progressively stripping off effects of the shallowest ensembles (or equivalent layers) and by correcting the power spectrum for source body width (Spector and Grant, 1970).

$$|A| = \sqrt{\left|\frac{dM}{dx}\right|^2 + \left|\frac{dM}{dy}\right|^2 + \left|\frac{dM}{dz}\right|^2} \quad (1)$$

The data were divided into six overlapping grid cells (Figure 4); each covering area extent of 10 km × 10 km and the corresponding radial power spectrum against wavenumber plots is depicted in Figure 5. The depths to the top (Z_t) and centroid depth (Z_o) of the magnetic source were obtained from the gradient of the high wavenumber portion and the slope of the low wavelength of the radially averaged power spectrum plots. The resultant depths of the radially averaged power spectrum are represented in Table 2. Horizontal ('x' and/or 'y') and vertical (z) dimensions and their corresponding geological models were obtained from Euler Deconvolution and are depicted in Figure 6. It delineates the geometry of magnetic bodies using the structural indices (SI) as discussed in Thompson (1982) and Barbosa et al. (1999). Structural index SI = 0 correspond contacts with 3 dimensions (peaks of block or solid rectangular shape), SI = 1 depicts intrusive bodies with 2 dimensions (sill or dike), SI = 2 gives penetrative horizontal cylinder or vertical bodies (pipes) and SI = 3 corresponds to a homogenous point source or sphere.

In order to normalize the signatures in the images, TDR and THDR were applied in such that weak, small amplitude anomalies were amplified relative to stronger ones. The THDR also defined the locations of magnetic edges, shows which side of each edge is likely to have a higher magnetization, and give a qualitative indication of the dip of contacts associated with TDR (the complement angle of the tilt angle). The basis of their definition is the total gradient of the magnetic field (Equation 1) and are related to angles derived from the gradients of the magnetic field (Fairhead and Williams, 2006) as stated in Eq. (2).

$$Tilt\ Derivative\ (TDR) = a\tan\frac{VDR}{THDR} \quad (2)$$

The suitability of these normalized magnetic derivatives in structural mapping is well known, and their interpretational meaning has been discussed in Miller & Singh (1994); Verduzco et al. (2004); Fairhead & Williams (2006); Fairhead et al. (2007); Salem et al. (2008). Sudden changes in the amplitude of a magnetic character may reflect boundaries between magnetic provinces, or a basement fault. The axes of continuous minima amplitude (weakly magnetized zones) on tilt derivative (TDR) and total horizontal derivative (THDR) maps in Figures 7a & 7b are traced as lineaments (Figure 8) to describe the trend within the magnetic units that indicates deformational trend (such as fractures, folds and fault patterns). From these derivative maps, the continuous zone of minima

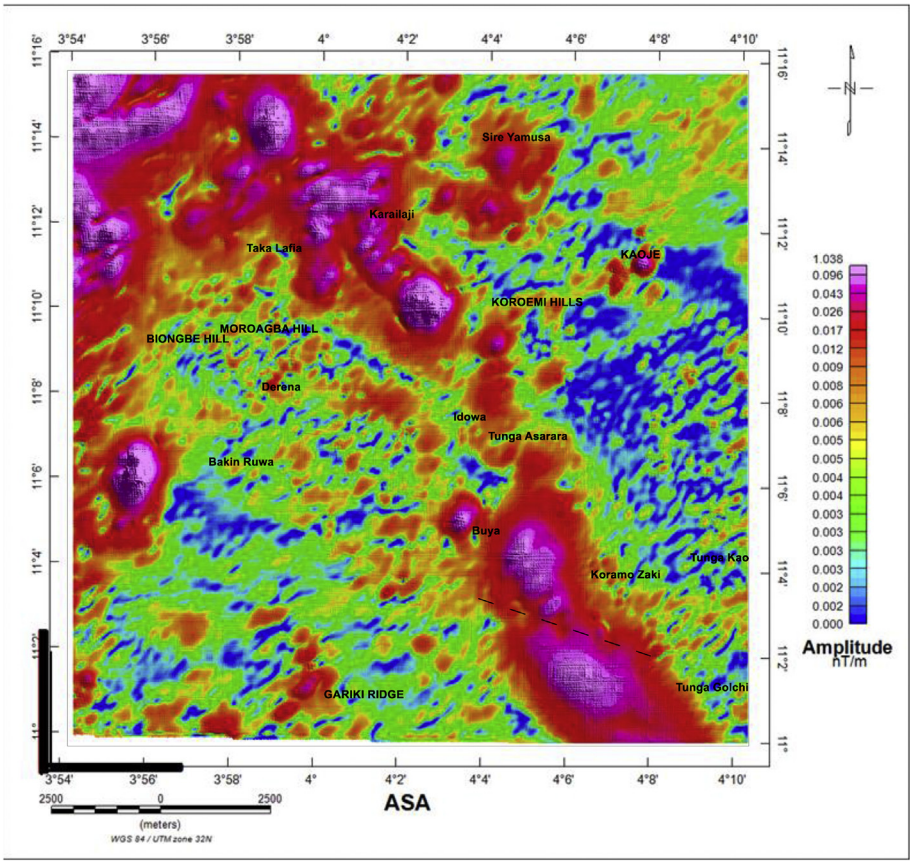


Figure 3. Analytic Signal Amplitude map.

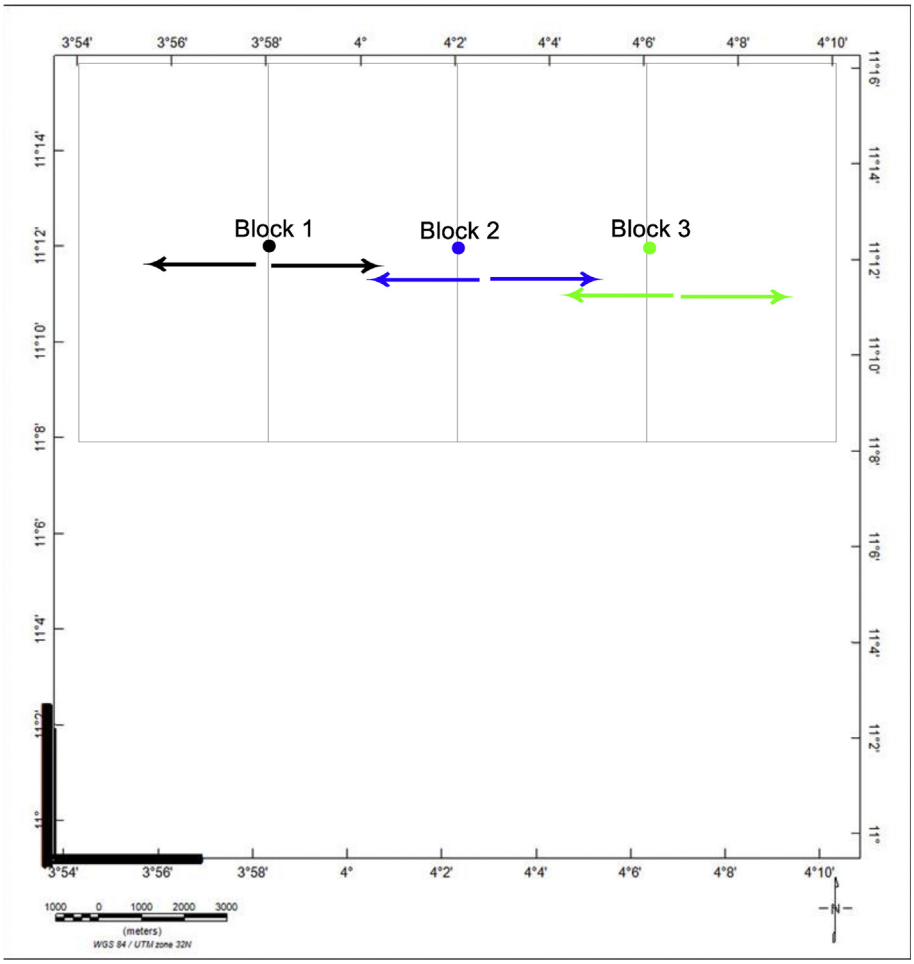


Figure 4. Description of Overlapping blocks from the aeromagnetic data; 10 km × 10 km grid blocks.

may as well represent either total field maxima or minima (Paananen, 2013).

3. Interpretations and discussion of results

The interpretation involved visual inspection and automated analysis of images, maps of aeromagnetic data and other relevant field investigation to define: boundaries of magnetic units; depth to magnetic sources; the geometry of lithologic units; mode of occurrence of the ores and; associated structural features. Complex information in the original data are simplified for improved understanding and useful litho-structural interpretation through filtering and analysis (Ajakaiye, 1981; Langel and Hinze, 1998; Blakely Simpson, 1986).

3.1. Lithologic mapping

The RTE residual anomaly map of the study region (Figure 2) generated from the high resolution aeromagnetic data generally simulates the earlier studied Cretaceous Sokoto sedimentary basin and the Basement Complex of Northwestern Nigeria. It exhibits negative to the positive magnetic intensity which range from -73.4 to 205.6 nT and depicts contrasting lithology of the sedimentary and Basement Complex rocks. The southeastern part of Garigi ridge section, the western axis of Koroemi ridge and Bakin-Ruwa and some sections of the northwestern region are characterized by negative magnetic anomalies (A, B, C, D, E, G) of intensity greater than or equal – 73.49 nT. The NW - SE trending negative anomalies are associated with rocks of the lower content of ferromagnetic minerals and are attributable to underlying igneous and metamorphic rocks or granitic intrusion while the intermediate positive magnetic anomalies Q1 and Q2 (having intensity range within 61.5–87.8 nT), coincide the undifferentiated Basement Complex rocks with predominant NE - SW quartz-mica schist. The anomaly Q2 has the same tone as Q1 and thus, is an update on the geometry of Zuru Schist Belt extension to the southern region of Kaoje. The positive high magnetic anomalies range within 89.51–205.63 nT, corresponds the prevalent sedimentary bedding viz; the sandstones, siltstones and claystone within Biongbe, Morongba and Koroemi hills in the upper half of the area and NNW-SSE trending goethite earlier reported by Bamigboye et al. (2018).

The maximum amplitude of the analytic signal (Figure 3) distinctly fall on the edges of the mapped sedimentary fabrics and intrusive contact within the schist belt. The AS peak showing NW-SE trending across low magnetic gradient coincide the NW-SE trending negative magnetic anomalies and low magnetic source depth; which suggests the intrusive body as generally steeply inclined across the Garigi and Koroemi ridges. The geologic field inspections validate the general NW-SE trend of contrasting lithologic units in the area. Exposed conical shape migmatite around Bakin-Ruwa and eastern axis of Buya, correspond the zones of high magnetic intensity (depicted with circles in Figure 2) and maximum analytic signal amplitude while the associated intrusive body (pegmatite) coincide low magnetic anomaly 'B'. The elongated banded gneiss within the schist body-mapped in Bamigboye et al. (2018), correspond the region of relatively high magnetic intensity that appears as crosscutting the intermediate anomalies Q1 and Q2 in southeast region of the area. Abrupt changes in magnetic units within the intermediate anomalies are

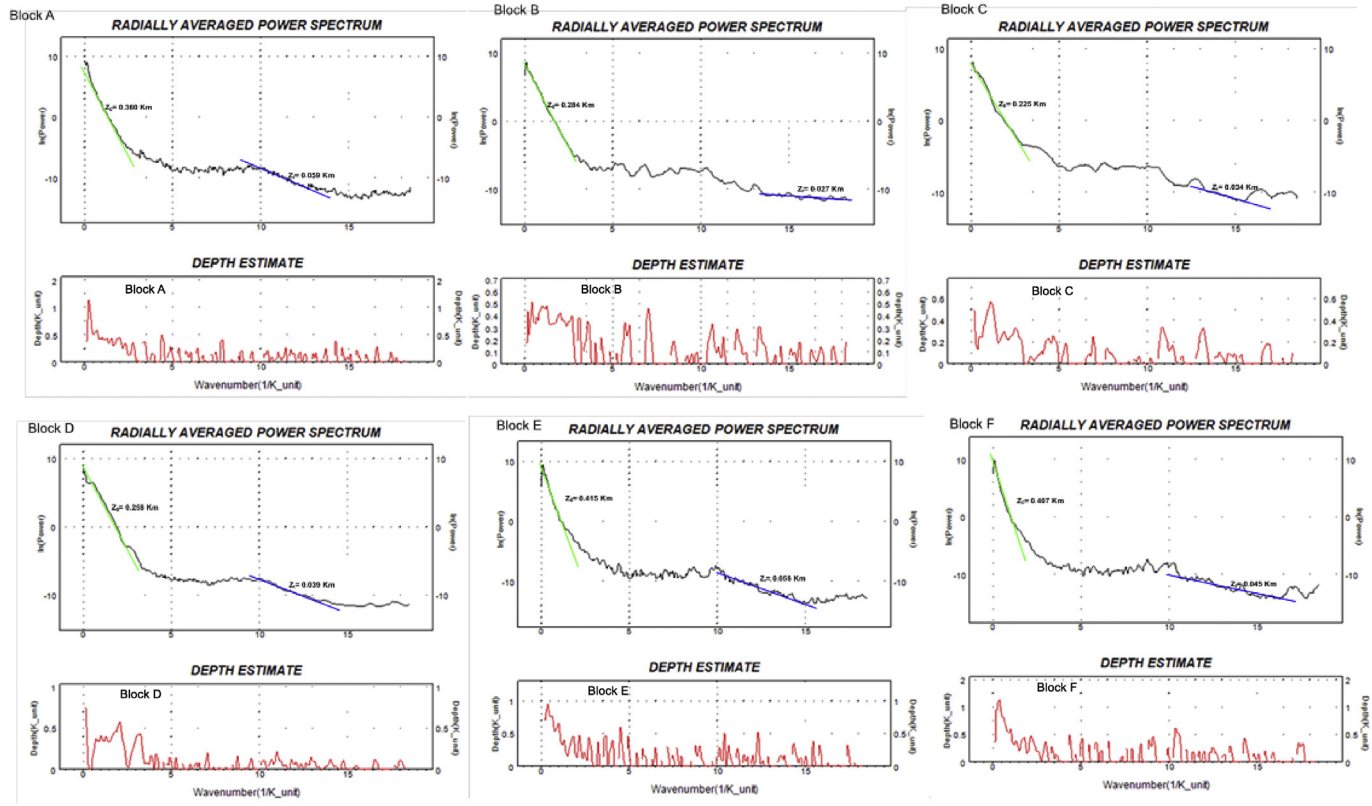


Figure 5. Radially averaged power spectrum and equivalent depth estimate; to the basement top (Z_t) and to deep source (Z_0) for overlapping grid cells of aeromagnetic data of Kaoje and its environ.

Table 2. Average depth estimate from radially power spectrum.

Overlapping Block	Region	location		Depth (m)	
		Easting	Northing	Z_t	Z_0
1	NW	3°58'	11°12'	59	360
2	N	4°2'	11°12'	27	284
3	NE	4°6'	11°12'	34	225
4	SW	3°58'	11°4'	39	258
5	S	4°2'	11°4'	58	415
6	SE	4°6'	11°4'	45	407
Average				43.7	324.8

associated with mapped fractures and joints which are filled by quartz and quartz-feldspathic veins or upward movement of iron through the overlying sediments.

The Euler solutions revealed perfect clustering along some notable anomalies; hence they are acceptable solutions for the associated geologic structures (Thompson, 1982; Reid et al., 1990; Feumoe *at al.*, 2012). The SI = 0, 1 (Figures 6a & 6b), distinctly revealed the contact and edges of the granitic body buried at a shallow depth less than 200 m while the SI = 2 (Figure 6c) corroborate the sandstone-hosted goethite mineralizations and schist hosted manganite depicted in rounded rectangle within northwest and southwest of Kaoje (west of Zuru schist belt). The SI = 3 (Figure 6d) revealed a corresponding sphere geologic model for the sandstone-hosted goethite mineralizations in the northwestern region of Kaoje at a depth range of 0–225 m. Estimated depth from radially averaged power spectrum ranged from 0 to 59 m and 225–415 m for shallow and deeper magnetic sources respectively, and agrees with the Euler depth solutions. Slopes of upper segments (green line) on the power spectrum plots (Figure 5) showing decreasing power as frequency increases, gives the deeper source depths while the gradients of the least descent (blue line) depict the shallowest depth estimate.

3.2. Structural mapping

Deformational features such as joints, faults, folds are often attributed to a sudden discontinuity of the magnetic unit, offsets of apparently similar magnetic units, an abrupt change in depth to magnetic sources, magnetic anomalies pattern and geometry of magnetic sources (Gunn et al., 1997). These geologic features are expressed with linear narrow magnetic low anomalies (associated with weathering) within magnetic highs or otherwise using normalized magnetic gradients (Fairhead et al., 2007; Salem et al., 2008; Paananen, 2013). The linear features are easily established on a grey shaded TDR map to corroborate THDR, since the human eye can clearly identify low band length range. Patterns of the linear amplitude of anomalies on the THDR and TDR maps show prominent NE-SW and NW-SE trend which is attributable to Pan African orogeny (600 Ma) and Kibaran Orogenic (1100 Ma) cycle of deformation (Burke and

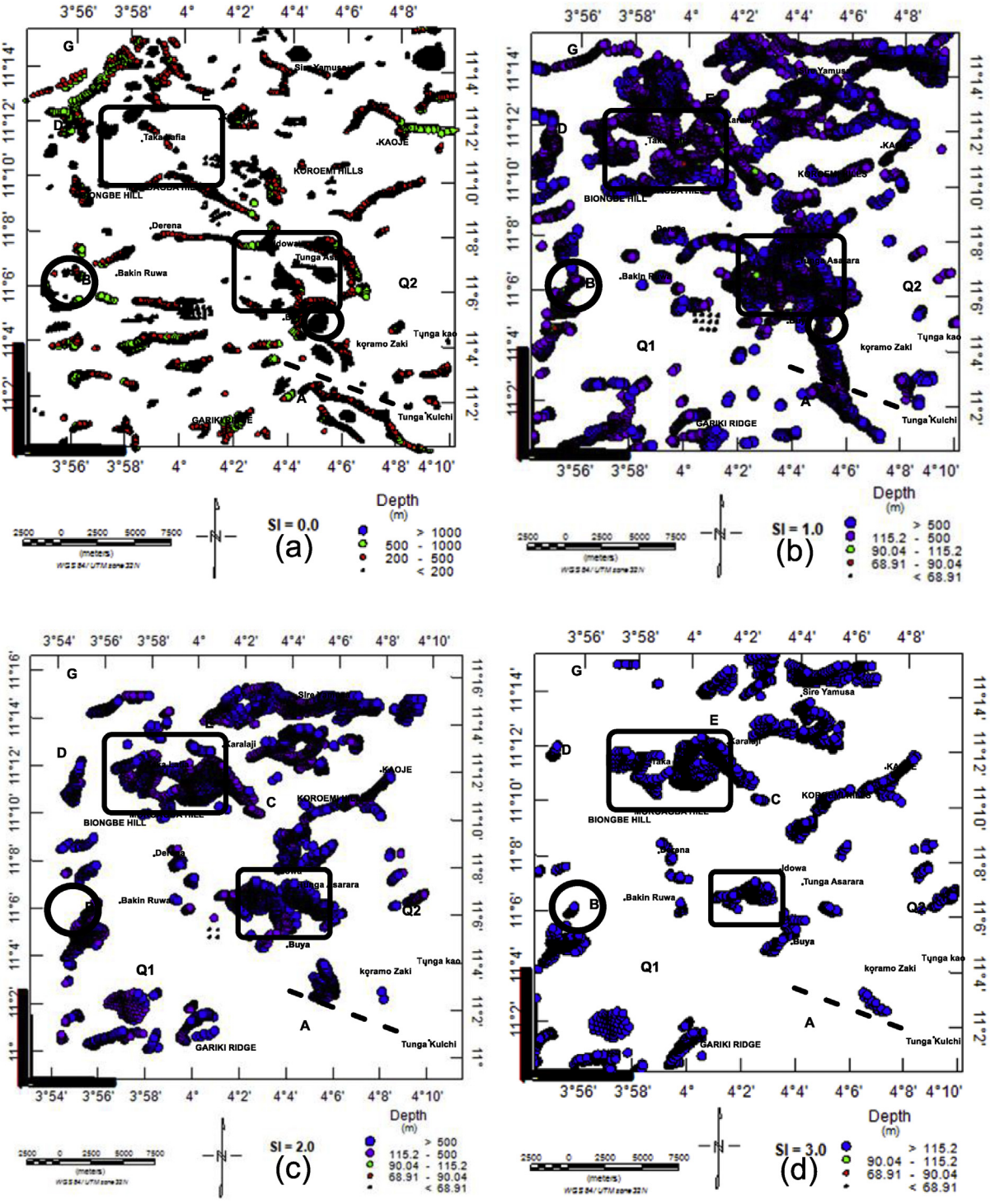


Figure 6. Euler deconvolution depth plots at different structural index SI (a) SI = 0; (b) SI = 1 (c) SI = 2 (d) SI = 3.

Dewey, 1972; Dada, 2006). The prominent trends are in concordance with the conspicuous magnetic anomalies and as such are classified as brittle deformation zones while the scanty linear/curvilinear E - W trends (in a purple circle) which crosscut the anomalies trends are ductile (Paananen, 2013; Oladunjoye et al., 2016). The late deformation could be responsible for the metamorphism, migmatisation, and gneissification near Bakin-Ruwa and Buya regions. Discontinuity in the extracted lineament (Figure 8) corresponds clockwise (sinistral) and anticlockwise (dextral) faults system. The sinistral fault (about 1 km wide at the SE) acts as a conduit for the granitic intrusion within the southeastern region (banded by the quartz-mica schist) and pegmatite around Bakin Ruwa. The extracted lineaments were superimposed on the reduced magnetic anomaly and geologic maps in Figures 9a and 9b respectively. These were used for appraisal of geologic settings and structural classification. The elongated fault in the northeast – north is attributable to an imprint of Zungeru-Anka transcurrent fault (Obaje, 2009) along Kaoje. This fault might be the channel conducting the FeMn mineralizing fluid to Kaoje and its environs.

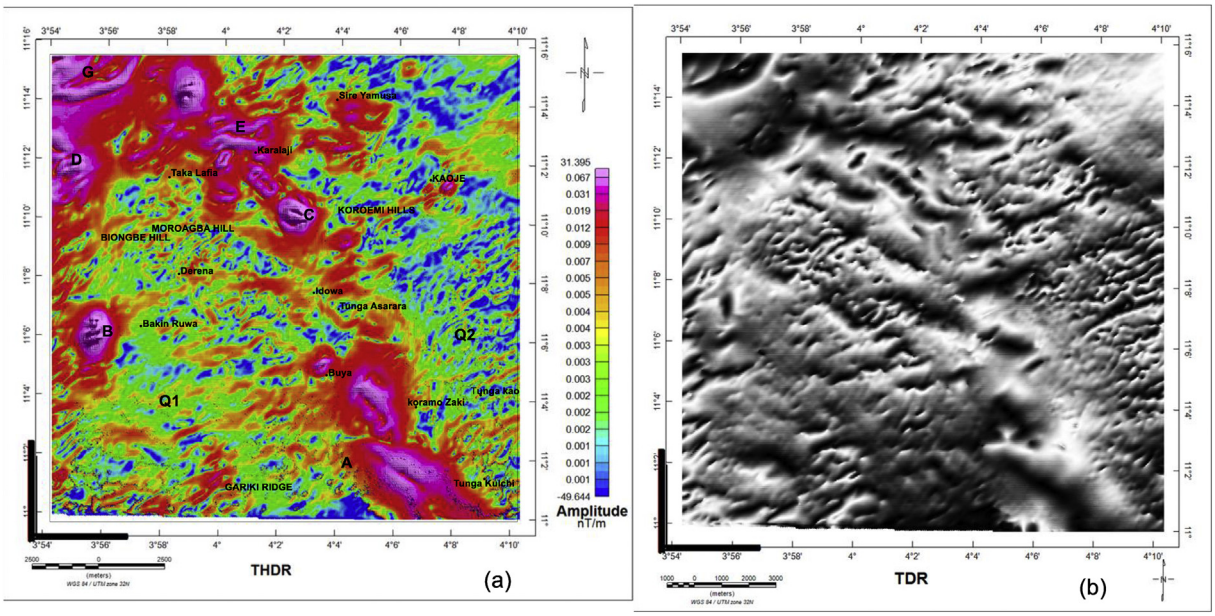


Figure 7. Derivative maps of reduced to equator residual magnetic intensity; (a) colored shaded THDR map and (b) grey scale TDR map.

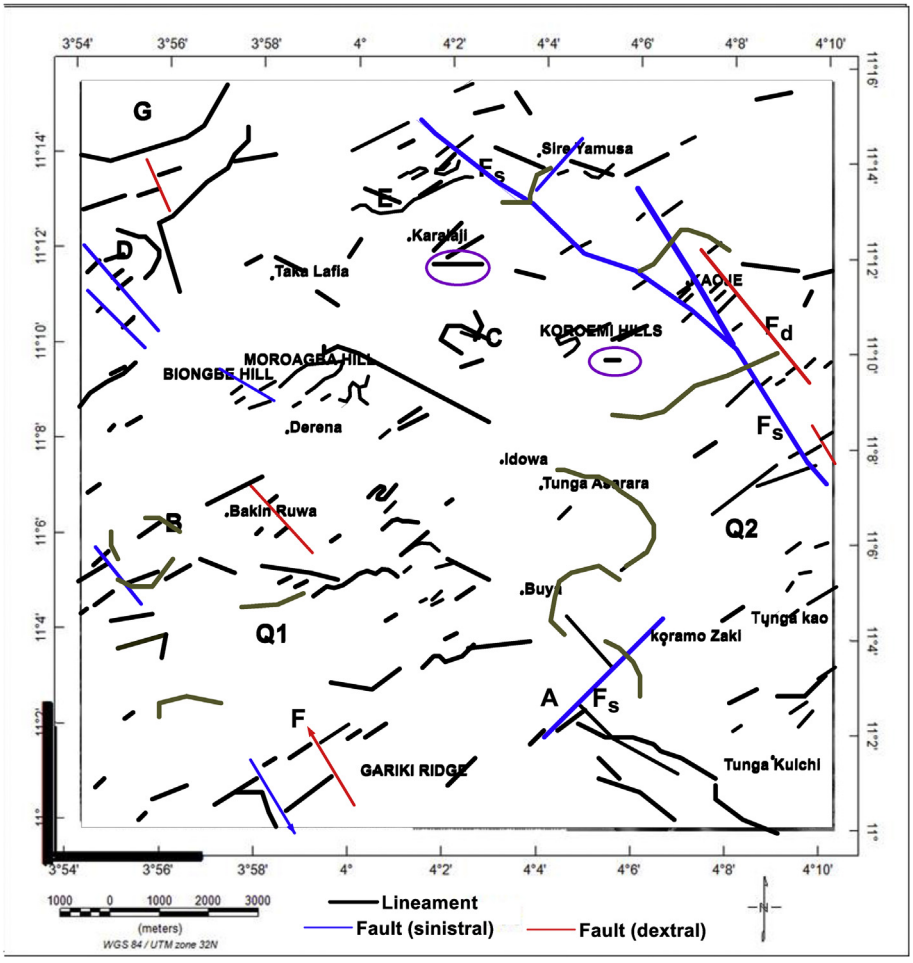


Figure 8. Lineaments extracted from total horizontal derivative (THDR), tilt derivative (TDR) and Euler deconvolution maps, showing the fractures and fault system of the area.

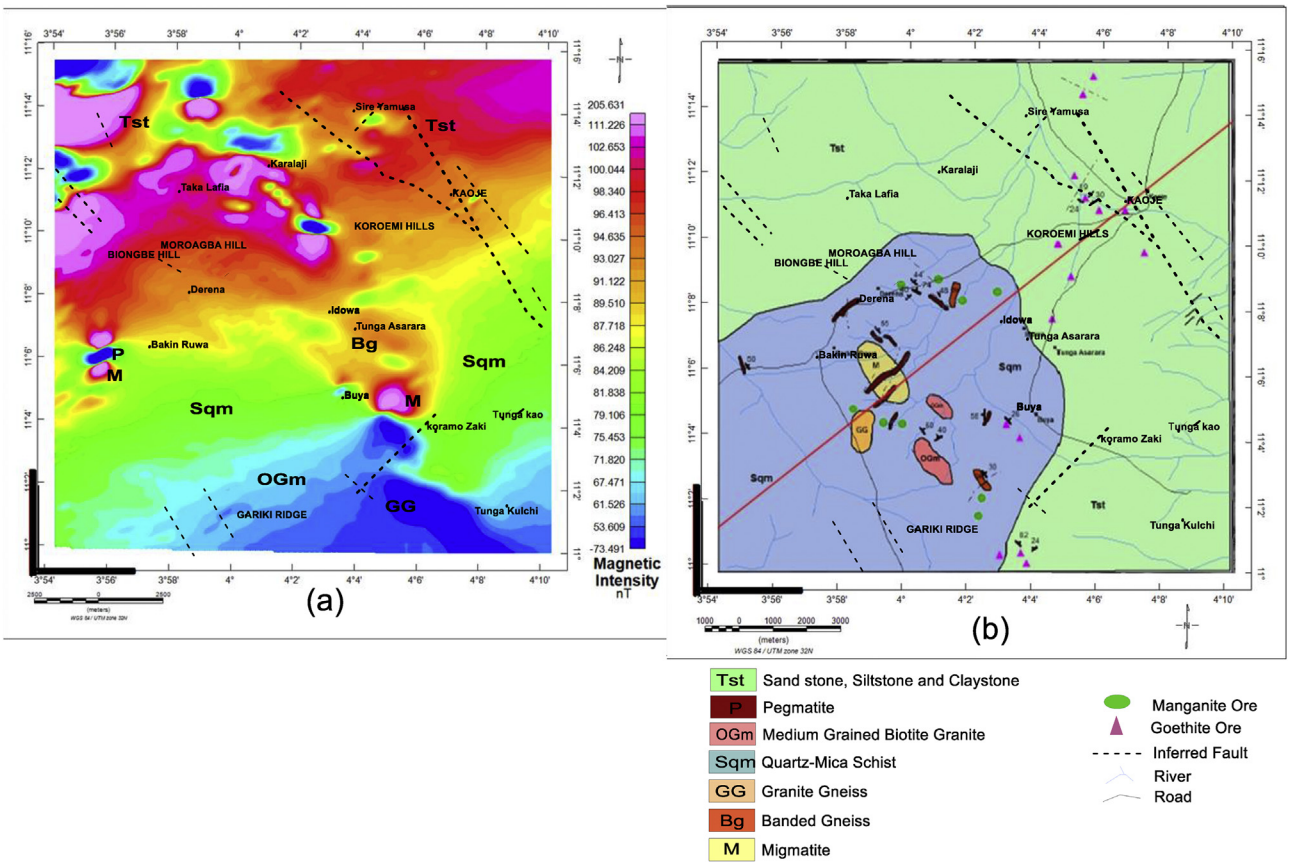


Figure 9. Inferred geologic structural map (a) magnetic anomaly and (b) updated geologic map.

4. Conclusion

From the results of interpretation of high-resolution aeromagnetic survey and geologic field mapping, the boundaries of magnetic units; depth to magnetic sources; the geometry of lithologic units; mode of occurrence of iron ores and; associated structural features of Kaoje and its environment were established. The reduced to equator residual magnetic intensity range from -73.4 to 205.6 nT and are associated with contrasting lithology of the sedimentary and Basement Complex rocks. The positive anomalies coincide with the prevalent sedimentary bedding and NNW-SSE trending goethite, the NW - SE trending negative anomalies are associated with underlying granitic rocks while the intermediate positive magnetic anomalies coincide the undifferentiated Basement Complex rocks with predominant NE - SW quartz-mica schist. The geologic features generally in concordance with the NE-SW and NW-SE structural trend, suggested the area has undergone varying tectonic events. The events protrude the imprint of Zungeru-Anka transcurrent fault that served as a conduit for iron mineralizing fluid to Kaoje and its environs. From the magnetic data, the lithologic units, the mode of occurrence and associated geologic features have been inferred and could be used to update the geology of the area. The iron mineralizations are concluded as sourced from the magmatic bodies that lie beneath the sedimentary rocks and a corresponding sphere geologic model within the northwest and southwest of Kaoje at a depth range of 0–225 m.

Declarations

Author contribution statement

Nurudeen Olasunkanmi, Olufemi Bamigboye: Conceived and designed the experiments; Performed the experiments; Analyzed and interpreted the data; Contributed reagents, materials, analysis tools or data; Wrote the paper.

Olatunji Saminu, Naheem Salawu, Toba Bamidele: Analyzed and interpreted the data; Contributed reagents, materials, analysis tools or data.

Funding statement

This research did not receive any specific grant from funding agencies in the public, commercial, or not-for-profit sectors.

Competing interest statement

The authors declare no conflict of interest.

Additional information

No additional information is available for this paper.

References

Ajakaiye, D.E., 1981. Geophysical investigation in the Benue trough – a review. Earth Evol. Sci. 1, 110–125.

Ajibade, A.C., Woakes, M., Rahaman, M.A., 1987. Proterozoic crustal development in the Precambrian regime of Nigeria. In: Kroner, A. (Ed.), Proterozoic Lithospheric Evolution, Geodynamics Series. American Geophysical Union, pp. 259–271.

Akande, S.O., Kinnaird, J., 1992. Characterization and origin of ore forming fluids in the Nigerian mineral belts. In: Maurice, Y. (Ed.), Symposium Vol. International Assoc. On the Genesis of Ore Deposits (I.A.G.O.D. Schweizerbatsche Press Stuttgart, pp. 199–218.

Akinlolu, F., 2007. Exploration and resource estimation of the manganese deposit in Kaoje, kebbi state. NGSA Report, p. 70p.

Amigun, J.O., Afolabi, O., Ako, B.D., 2012. Application of airborne magnetic data to mineral exploration in the okene iron ore province of Nigeria. Int. Res. J. Geol. Min. 2 (6), 132–140.
Ayodeji, J., Dare, O., 2015. Geological and structural interpretation of ado-ekiti southwest and its adjoining areas using aeromagnetic data. AAPG, SEG and SEPM Joint Technical Conference. AAPG, Oxnard, California.
Bamigboye, O.S., Adekeye, J.I.D., Omorinoye, O.A., Adedoyin, A.D., Adefila, I., 2015. Soil geochemical survey of Kaoje and environs. Sci. Focus 20 (1), 53–69.
Bamigboye, O.S., Adekeye, J.I.D., Kadioglu, Y.K., Adedoyin, A.D., Omorinoye, O.A., 2018. Geochemistry and origin of Fe-Mn oxide mineralization in Kaoje-Derena and their environs, northwestern Nigeria. Arabian J. Geosci. 11, 570–588.
Baranov, V., 1957. A new method for interpretation of aeromagnetic maps. Geophysics 359–383.
Barbosa, V.C.F., Silva, J.B.C., Medeiros, W.E., 1999. Stability analysis and improvement of structural index estimation in Euler deconvolution. Geophysics 64, 48–60.
Barton, M.D., Johnson, D.A., 2000. Alternative brine sources for Fe-oxide (-Cu-Au) systems: implications for hydrothermal alteration and metals. In: Porter, T.M. (Ed.), Hydrothermal Iron Oxide Copper-Gold and Related Deposits: A Global Perspective. Australian Mineral Foundation, Adelaide, pp. 43–60.
Bassey, C., Eminue, O., 2014. Preliminary evaluation of major and trace elements content of cretaceous – palaeogene formation of the Sokoto basin, northwestern Nigeria. NAFTA 65 (1), 69–76.
Blakely, R.J., Simpson, R.W., 1986. Locating edges of source bodies from magnetic and gravity anomalies. Geophysics 51 (7), 1494–1498.
Burke, K.C., Dewey, J.F., 1972. Orogeny in africa. In: Dessauvagie, T.F., Whiteman, A.J. (Eds.), Africa Geology. University of Ibadan Press, Ibadan, pp. 583–608.
Chapin, D.A., Yalamanchili, S.V., Daggett, P.H., 1998. The St. George Basin, Alaska COST#1 well: an example of the need for integrated interpretation. Geol. Appl. Grav. Magn. 49–51.
Dada, S.S., 2006. Proterozoic evolution of Nigeria. In: Oshi, O. (Ed.), The Basement Complex of Nigeria and its mineral Resources (A Tribute to Prof. M. A. O. Rahaman). Akin Jinad & Co. Ibadan, pp. 29–44.
Danbatta, U.A., Garba, M.L., 2007. Geochemistry and petrogenesis of Precambrian amphibolites in the Zuru schist belt, northwestern Nigeria. J. Min. Geol. 43 (1), 23–30.
Foss, C., 2011. Magnetic data enhancement and depth estimation. In: Gupta, H.K. (Ed.), Encyclopedia of Solid Earth Geophysics. Springer Science+Business Media B.V.
Fairhead, J.D., Williams, S.E., 2006. Evaluating Normalized Magnetic Derivatives for Structural Mapping. SEG 2006 New Orleans Extended Abstract. SEG.
Fairhead, D., Williams, S., Ben, S.A., 2007. Structural Mapping from High Resolution Aeromagnetic Data in Namibia Using Normalized Derivatives. Innovation in EM, Grav and Mag Methods:a New Perspective for Exploration. EGM 2007 International Workshop, Capri, Italy.
Feumoe, A.N.S., Ndougsa-Mbarga, T., Manguelle-Dicoum, E., Fairhead, J.D., 2012. Delineation of tectonic lineaments using aeromagnetic data for the south-east Cameroon area. Geofizika 29 (2), 175–192.
Fillie, S., 2014. Genesis and Paragenesis of the Tetravalent Mn Ores and Mn-Fe Ores in Secondary Banded Iron Formations from Nigeria. Proceedings of the 3rd World Conference on Applied Sciences. Engineering and Technology, Kathmandu, Nepal, pp. 318–328.
Geosoft, 2005. Quick Start Tutorial and User Guide Applications (Electronic Version); Oasis Montaj Data Processing and Analysis (DPA) System for Earth Science Applications. Euro Technologies, p. 63.
Gunn, P.J., FitzGerald, D., Yassi, N., Dart, P., 1997. New algorithms for visually enhancing airborne geophysical data. Explor. Geophys. 28 (2), 220.
Ibrahim, W.S., Watanabe, K., Yonezu, K., 2016. Structural and litho-tectonic controls on Neoproterozoic base metal sulfide and gold mineralization in North Hamisana shear zone,South Eastern Desert, Egypt: the integrated field, structural,Landsat 7 ETM+ and ASTER data approach. Ore Geol. Rev. 79, 62–77.
Keating, P., 1995. A simple technique to identify magnetic anomalies due to kimberlite pipes. Explor. Minning Geol. 121–125.
Langel, R.A., Hinze, W.J., 1998. The Magnetic Field or the Earth's Lithosphere: the Sattelite Perspective. Cambridge University Press.
Macnae, J.C., 1979. Kimberlites exploration. Geophysics 1395–1416.
Miller, H.G., Singh, V., 1994. Potential Field Tilt – a new concept for location of potential field sources. J. Appl. Geophys. 213–217.
Nabighian, M.N., 1972. The analytic signal of two-dimensional magnetic bodies with polygonal cross-section: its properties and use for automated anomaly interpretation. Geophysics 507–517.
NGSA, 2006. Goelogical and Mineral Resources Map of Kwara State, Nigeria. Nigeria Geological Survey Agency, Abuja.
Nureddin, M.S., Koichiro, W., Akira, I., Hakim, S., 2008. Integrating potential fields with remote sensing data for geological investigations in the Eljufra area of Libya. Earth Planets Space 539–547.
Nwankwo, L.I., Shehu, A.T., 2015. Evaluation of Curie-point depths, geothermal gradients and near surface heat flow from high-resolution aeromagnetic (HRAM) data of the entire Sokoto Basin, Nigeria. J. Volcanol. Geoth. Res. 45–55.
Obaje, N.G., 2009. Geology and mineral resources of Nigeria. Lecture Notes in Earth Sciences. Springer, Berlin Heidelberg.
Oladunjoye, M.A., Olayinka, A.I., Alaba, M., Adabanija, M.A., 2016. Interpretation of high resolution aeromagnetic data for lineaments study and occurence of banded iron formation in Ogbomoso area, Southwestern Nigeria. J. Afr. Earth Sci. 43–53.
Olasunkanmi, N.K., Olufemi, S.B., Aina, A., 2017. Exploration for iron ore in agbado-okudu, kogi state, Nigeria. Arab. J. Geosci. 10 (541).
Paananen, M., 2013. Completed Lineament Interpretation of the Oikiluoto Region. Posiva, 2013.
Patterson, N.R., Reeves, C.V., 1985. Effects of the equitorial electrojet on aeromagnetic data acquisition. J. Int. Geophys. 55.
Power, M., Belcourt, G., Rockel, E., 2004. Geophysical Methods for Kimberlite Exploration in Northan Canada. The Leading Edge, p. 1124.
Reid, A.B., Allsop, J.M., Granser, H., Millett, A.J., Somerton, I.W., 1990. Magnetic interpretation in three dimensions using Euler deconvolution. Geophysics 80–91.
Roest, W.R., Verhoef, J., Pilkington, M., 1992. Magnetic interpretation using the 3-D analytic signal. Geophysics 57 (1), 116–125.
Roux, G.M., 1970. The application of geophysics to gold exploration in South Africa. Minning Groundw. Geophys. 425–438.
Salem, A., Williams, S., Fairhead, D., Smith, R., Dhananjay, R., 2008. Interpretation of magnetic data using tilt-angle derivatives. Geophysics 73, L1–L10.
Spector, A., Grant, F.S., 1970. Statistical models for interpreting Aeromagnetic data. Geophysics 293–302.
Thompson, D.T., 1982. EULDPH-new technique for making computer-assisted depth estimates from magnetic data. Geophysics 31–37.
Thurston, J.B., Guillon, J.C., Smith, R.S., 1999. Model Independent Depth Estimation with the SPITM Method. *69th Annual International Meeting*. Society of Exploration Geophysics, pp. 403–406.
Verduzco, B., Fairhead, J.D., Green, C.M., MacKenzie, C., 2004. New insights into magnetic derivatives for structural mapping. Lead. Edge 116–119.